Supplementary Information Inventory

1. Extended Experimental Procedures
2. Three (3) supplementary figures and associated legends
3. One (1) Table

EXTENDED EXPERIMENTAL PROCEDURES

Protein Preparation

The *cesAB* and *espA* genes encoding the wild type CesAB (B7UMC4_ECO27) and the wild type EspA (B7UM94_ECO27) were isolated and cloned as described previously (Chen et al., 2011). The ATPase *escN* encoding EscN (B7UMA6_ECO27) was isolated by PCR from cosmid pCVD462 (a gift from Dr. J.B. Kaper) derived from the locus of enterocyte effacement (LEE) of E2348/69 cloned into pCVD551 (McDaniel and Kaper, 1997) and were finally cloned into pET16b. The mutants were constructed by site-directed mutagenesis using PfuUltraTM High Fidelity DNA polymerase (Quick-Change; Stratagene). The constructs were transformed in BL21(DE3) cells and grown at 37 °C, and protein synthesis was induced by addition of 0.5 mM of IPTG at A_{600} ~0.4. Isotopically labeled samples for NMR studies were prepared by growing the cells in minimal (M9) medium. Cells were harvested at A_{600} ~1.5 for LB media and A_{600} ~1.0 for M9 media. U-[^{2}H/^{15}N/^{13}C]-labeled sample was prepared for the backbone assignment by supplementing the growing medium with 1 g L^{-1} of $^{15}NH_4Cl$ and 2 g L^{-1} of $^{2}H_7$,$^{13}C_6$-glucose in 99.9%-$^{2}H_2O$ (CIL). The methyl-protonated samples were prepared as described (Gelis et al., 2007). 50 mg L^{-1} of alpha-ketobutyric acid and 85 mg L^{-1} of alpha-ketoisovaleric acid were added to the culture 45 min prior to addition of IPTG. Met-[$^{13}CH_3$] and Ala-[$^{13}CH_3$] labeled samples were produced by supplementing the medium with 100 mg L^{-1} of [$^{13}CH_3$]-methionine and 100 mg L^{-1} [$^{2}H_2$,$^{13}CH_3$]-alanine as described (Popovych et al., 2009). All protein samples were purified over a nickel-chelating Sepharose column (GE Healthcare), followed by a Superdex-75 size exclusion column (GE Healthcare).

CesAB–EspA Selective Isotope Labeling by In Vitro Reconstitution.

Purified unlabeled His-CesAB–EspA and isotopically labeled His-CesAB–EspA samples were denatured by using 8 M urea solution. The two proteins in the complex were separated by nickel-chelating Sepharose column (GE Healthcare) under denatured condition. Isotope-labeled or unlabeled CesAB was mixed with unlabeled or isotope-labeled EspA, respectively, in 1:1 molar ratio under denatured condition to yield differentially labeled protein in the complex. The proteins in the mixtures were refolded by 25 times dilution into refolding buffer (50 mM Tris, pH 7.5, 100 mM NaCl and 5% glycerol). Excess urea was removed by extensive dialysis with an Amicon stirred cell.

NMR Spectroscopy

NMR experiments were performed on Varian 600 and 800 MHz and Bruker 600 and 700 MHz spectrometers. Sequential assignment of the ^{1}H, ^{13}C, and ^{15}N protein backbone chemical shifts

was achieved by means of through-bond heteronuclear scalar correlations with standard pulse sequences. NMR samples for CesAB were prepared in 300 mM KCl, 50 mM potassium phosphate, 1 mM DTT, and 1 g L^{-1} NaN3 (pH 6.5). Samples for CesAB–EspA complex were prepared in 50 mM KCl, 50 mM potassium phosphate, 1 mM DTT, and 1 g L^{-1} NaN3 (pH 7.0). Samples for the EscN titration experiments were prepared in 50 mM KCl, 100 mM potassium phosphate, 5 mM DTT, 0.5 mM EDTA and 1 g L^{-1} NaN3 (pH 7.5). Spectra were recorded at 26 ºC for CesAB samples, 37 ºC for CesAB–EspA samples and 25 ºC for all the EscN related experiments. All spectra were processed using NMRPipe (Delaglio et al., 1995).

Structure Determination Protocol

The structure of CesAB^{S} was calculated with CNS (Brunger, 2007), within ARIA 1.2 (Linge et al., 2003). The $^{13}C\alpha$, $^{13}C'$, Hα, ^{15}N, and NH chemical shifts served as input for the TALOS program (Shen et al., 2009) to extract dihedral angles (φ and ψ). The Distance restraints derived from the NOESY spectra were with upper-bound distances of 5.0 Å. Several set of hydrogen bond restraints were included for amides located in helices, as determined via NOE data and chemical shift information. The initial structure of the monomer was used to dock two monomers into a homodimer of CesAB^{S} driven by inter-molecular NOEs. The docking protocol consisted of three stages: (i) randomization of orientations and rigid body energy minimization generating a set of 1000 structures; (ii) the best 100 solutions according to CNS rigid body score were selected for semi-flexible refinement in torsion angle space; and (iii) the structures were finally refined in explicit water. A simulated annealing protocol was used using both torsion angle dynamics and Cartesian dynamics.

Circular Dichroism Spectroscopy

CD spectra acquired in the near-UV region monitor the local asymmetry of aromatic residues and are a sensitive diagnostic probe of protein tertiary structure. Near-UV CD measurements were performed on an Aviv Model 400 CD Spectropolarimeter (Aviv Biomedical, Inc., Lakewood, NJ) routinely calibrated with 10-camphorsulfonic acid at 290.5 nm (Zhong and Johnson, 1992). Standard solutions of wild type CesAB homodimer and the CesAB^{S} construct were prepared at a total protein concentration of 100 µM in a buffer system consisting of 50 mM potassium phosphate, 100 mM potassium chloride, 0.5 mM EDTA, and 5.0 mM DTT adjusted to pH 7.5. Protein samples were transferred to 1.0 cm quartz cuvettes and equilibrated at 0 ºC for 30 minutes prior to optical analysis. The conformation of each protein was evaluated by recording the ellipticity over the wavelength range of 250 to 350 nm at 0.5 nm increments following

signal averaging for 30 seconds. The resultant CD spectra were buffer subtracted and concentration normalized to yield mean residue ellipticity [θ] in units of deg•cm^2•dmol^{-1} as calculated from the following relation:

$$[\theta] = ([\theta]_{obs} \times MRW) / (10 \times l \times c)$$

where $[\theta]_{obs}$ is the observed ellipticity in degrees, MRW is the mean residue molecular weight (molecular weight of the protein divided by the number of backbone amides), l is the optical path length of the cuvette in cm, and c is the protein concentration in g mL^{-1}.

In Vivo Secretion from EPEC Strains.

In vivo secretion was induced by incubation of EPEC strain cultures at 37°C in LB medium. All genes of interest were cloned downstream from the Tet promoter and the expression of these genes was induced by addition of 0.1 μg mL^{-1} of unhydro-tetracycline (IBA, Germany) to the culture when OD_{600} reached 0.3. Total cells and supernatant fractions were separated by centrifugation for 10 min at 4,000 x g at 4 ºC at different time intervals. Proteins in the spun growth medium were precipitated with trichloacetic acid (20 % w/v; 30 min; 4 ºC) followed by two ice-cold acetone washes. Finally the secreted polypeptides were analyzed by 15% SDS-PAGE and immunoblotting using rabbit polyclonal antibodies against EspA. Polypeptides were quantified using a CCD camera (LAS 3000, FujiFilm) and Image J open software (version 64, available on-line at http://rsbweb.nih.gov/ij/download.html) and a standard curve of purified proteins.

Infection of HeLa Cells

Bacterial cultures of EPEC strains were grown for 18 h in LB medium, and then were diluted 100-fold in DMEM medium and allowed to grow for another 3 h at 37 ºC, 5% CO_2 without shaking for the priming of bacteria. The sub-confluent lawns of HeLa cells, which had grown on glass coverslips inside a 24-well tissue culture dish (approximately 40,000 cells per well), were infected for 2 h, unless otherwise indicated, with the primed bacterial cultures (~3.5 x 10^7 bacteria were inoculated in each well). The non-adhered bacteria were removed with sequential gentle washes with 1 x PBS solution and the cells were fixed with 3% Paraformaldehyde (PFA) for 30 min. After removal of PFA, cells were permeabilized with 0.1% TRITON X-100. After incubation with a polyclonal α-EspA antibody (500-fold dilution; 30 min), cells were rinsed 3 times and the EspA filaments were stained with a donkey α-rabbit (200-fold dilution; Cy3-labeled, Jackson Immunoresearch). In parallel, the eukaryotic actin was detected

with phalloidin (Cy2-labeled, Invitrogen) and both DNA bacterial and eukaryotic DNAs were stained with 1/1000 TOP-RO-3 solution (Invitrogen). The Coverslips were mounted on slides using Prolong Gold anti-fade reagent (Invitrogen) and were examined with an Axio Imager M1 Microscope (Carl Zeiss MicroImaging GmbH, Germany). Finally the images were acquired using an AxioCam MRm monochrome camera and computer processed using Axiovision software (Carl Zeiss MicroImaging GmbH, Germany).

SUPPLEMENTAL REFERENCES

Brunger, A.T. (2007). Version 1.2 of the Crystallography and NMR system. Nat Protoc *2*, 2728–2733.

Delaglio, F., Grzesiek, S., Vuister, G., Zhu, G., Pfeifer, J., and Bax, A. (1995). NMRPipe: a multidimensional spectral processing system based on UNIX pipes. J Biomol NMR *6*, 277–293.

Gelis, I., Bonvin, A.M.J.J., Keramisanou, D., Koukaki, M., Gouridis, G., Karamanou, S., Economou, A., and Kalodimos, C.G. (2007). Structural basis for signal-sequence recognition by the translocase motor SecA as determined by NMR. Cell *131*, 756–769.

Linge, J.P., Habeck, M., Rieping, W., and Nilges, M. (2003). ARIA: automated NOE assignment and NMR structure calculation. Bioinformatics *19*, 315–316.

Popovych, N., Tzeng, S.-R., Tonelli, M., Ebright, R.H., and Kalodimos, C.G. (2009). Structural basis for cAMP-mediated allosteric control of the catabolite activator protein. Proc Natl Acad Sci USA *106*, 6927–6932.

Shen, Y., Delaglio, F., Cornilescu, G., and Bax, A. (2009). TALOS+: a hybrid method for predicting protein backbone torsion angles from NMR chemical shifts. J Biomol NMR *44*, 213–223.

Zhong, L., and Johnson, W.C. (1992). Environment affects amino acid preference for secondary structure. Proc Natl Acad Sci USA *89*, 4462–4465.

FIGURE LEGENDS

Figure S1. Structural Characterization of CesAB^s, Related to Figure 1

(A) and (B) Overlaid ^{1}H-^{15}N HSQC and ^{1}H-^{13}C HMQC spectra of CesAB and CesAB^s. The dramatic improvement in resonance dispersion indicates that, in contrast to CesAB, CesAB^s is a well folded protein.

(C) and (D) Far-UV and near-UV CD data of CesAB and CesAB^s demonstrate that the helicity is substantially enhanced and aromatic packing is greatly improved in CesAB^s.

(E) Solution structure of CesAB^s. The ensemble of the 20-lowest energy conformers of CesAB^s is shown. Two orthogonally-related views of CesAB^s of the lowest-energy conformer with residues mediating the dimer displayed as yellow sticks are also shown.

(F) Superposition of the structures of CesAB^s and wild-type CesAB.

(G) Superposition of the structures of CesAB^s and CesAB–EspA.

Figure S2. Interaction of Hexameric EscN with CesAB, CesAB–EscN and CesAB^{s}, Related to Figure 2.

(A) Size exclusion chromatography of EscN. At concentrations higher than ~20 μM, EscN exists as a hexamer in solution.

(B) Size exclusion chromatography of EscN$^{\Delta N}$, a variant that lacks the N-terminal region (residues 1-97) and exists exclusively as a monomer in solution.

(C) ATPase activity of EscN, EscN-R366D, and EscN$^{\Delta N}$. Arg366 plays the role of the so-called "arginine finger" residue, which is required for stimulation of the ATPase activity. Arg366 from a different subunit is thought to poke into the ATP-binding pocket when EscN forms functional oligomers (Zarivach et al., 2007). No detectable ATPase activity was measured for EscN-R366D and EscN$^{\Delta N}$. The profile for EscN-R366D is slightly offset for clarity.

(D) Overlaid ^{1}H-^{13}C HMQC spectra of CesAB in the absence (blue) and presence (red) of EscN. No binding was detected. Due to the poor sensitivity of the ^{1}H-^{15}N HSQC spectrum of CesAB (Figure 1E) the side-chain methyl spectrum, wherein all expected peaks are present, was used to probe for the interaction.

(E) Overlaid ^{1}H-^{15}N HSQC spectra of CesAB–EspA in the absence (green) and presence (red) of EscN. The data indicate formation of the ternary CesAB–EspA–EscN complex. Several residues of the CesAB–EspA complex are unaffected by EscN binding. All these residues are located in flexible regions of the heterodimer that are not immobilized upon formation of the ternary complex.

(F) Overlaid ^{1}H-^{15}N HSQC spectra of CesAB–EspA in the absence (green) and presence (orange) of EscN$^{\Delta N}$. The data show that there is no interaction between the two proteins.

(G) Overlaid ^{1}H-^{15}N HSQC spectra of CesAB^{s} in the absence (purple) and presence (red) of EscN indicating binding. The residues that are not affected by EscN binding are located in the flexible C-terminal tail of CesAB.

(H) Residues identified by NMR to mediate the interaction of CesAB^{s} with EscN.

(I) Residues identified by NMR to mediate the interaction of CesAB–EspA with EscN. The EscN-binding surfaces in CesAB–EspA and CesAB^{s} are very similar and consist in both cases of helices 2 and 3 of CesAB.

(J) Overlaid ^{1}H-^{15}N HSQC spectra of EspA$^{1-34}$ in the absence (blue) and presence (orange) of EscN. No binding was detected.

(K) Overlaid ^{1}H-^{15}N HSQC spectra of CesAB–EspA (green) and CesAB–EspA$^{\Delta 29}$ (orange). Truncation of the N-terminal 29 residues of EspA does not affect the fold of the heterocomplex and has a minimal effect on its structure.

(L) Overlaid ^{1}H-^{15}N HSQC spectra of CesAB–EspA$^{\Delta 29}$ in the absence (green) and presence of EscN (red). Truncation of the N-terminal 29 residues of EspA does not abrogate binding of CesAB–EspA$^{\Delta 29}$ to EscN.

Figure S3. EspA secretion is dependent on the presence of the EscN ATPase, Related to Figure 3.

In vivo infection of HeLa cells in wild-type and Δ*escN* strains. EscN deletion results in complete abrogation of EspA secretion and therefore no infection is observed after 120-min inoculation with bacteria.

TABLES

Table S1 NMR and refinement statistics for CesAB^{s} structure

NMR Restraints (per subunit)	
Distance restraints	
NOEs	331
Sequential (|i-j|=1)	126
Medium range (1<|i-j|<4)	70
Long range (|i-j|>4)	116
Inter-subunit	19
Hydrogen bonds	130
Paramagnetic relaxation enhancement rates	52
Total Dihedral angle restraints	268
φ	134
ψ	134
Structure statistics (15 structures)	
Violations (mean and SD)	

Distance restraints (Å)	0.22 ± 0.02
Dihedral angle restraints (°)	4.0 ± 0.39
Deviations from idealized geometry	
Bond lengths (Å)	0.004
Bond angles (°)	0.5
Impropers (°)	1.3
Ramachandran plot statistics* (%)	
Residues in most favored regions	98.6
Residues in additionally allowed regions	1.3
Residues in generously allowed regions	0.1
Residues in disallowed regions	0.0
Average pairwise rmsd* (Å)	
Backbone	1.2
Heavy atoms	1.4

*Statistics applied to residues 1-85 (the region encompassing residues 86-107 is unstructured)

Supplemental Figure 1

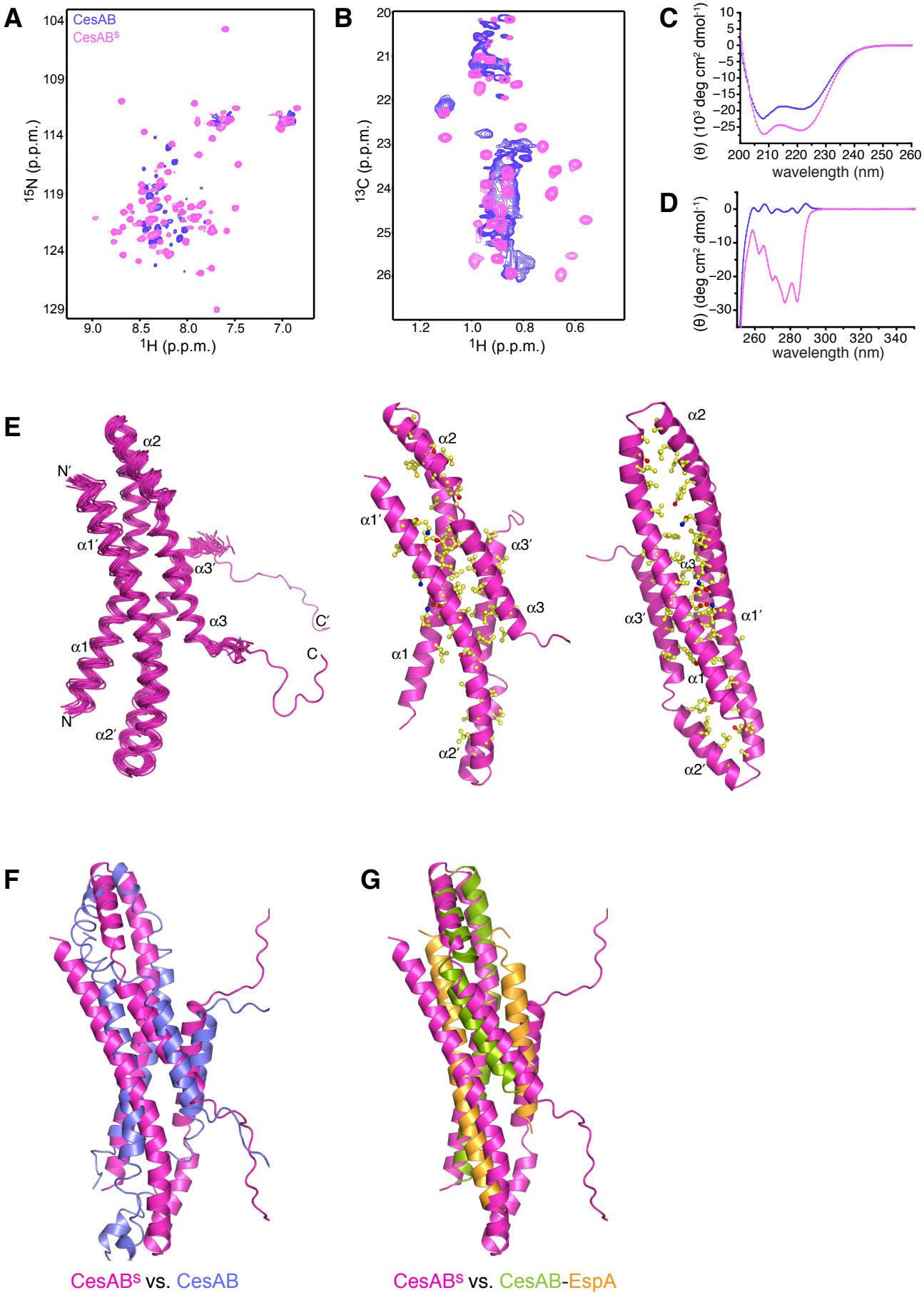

Supplemental Figure 2

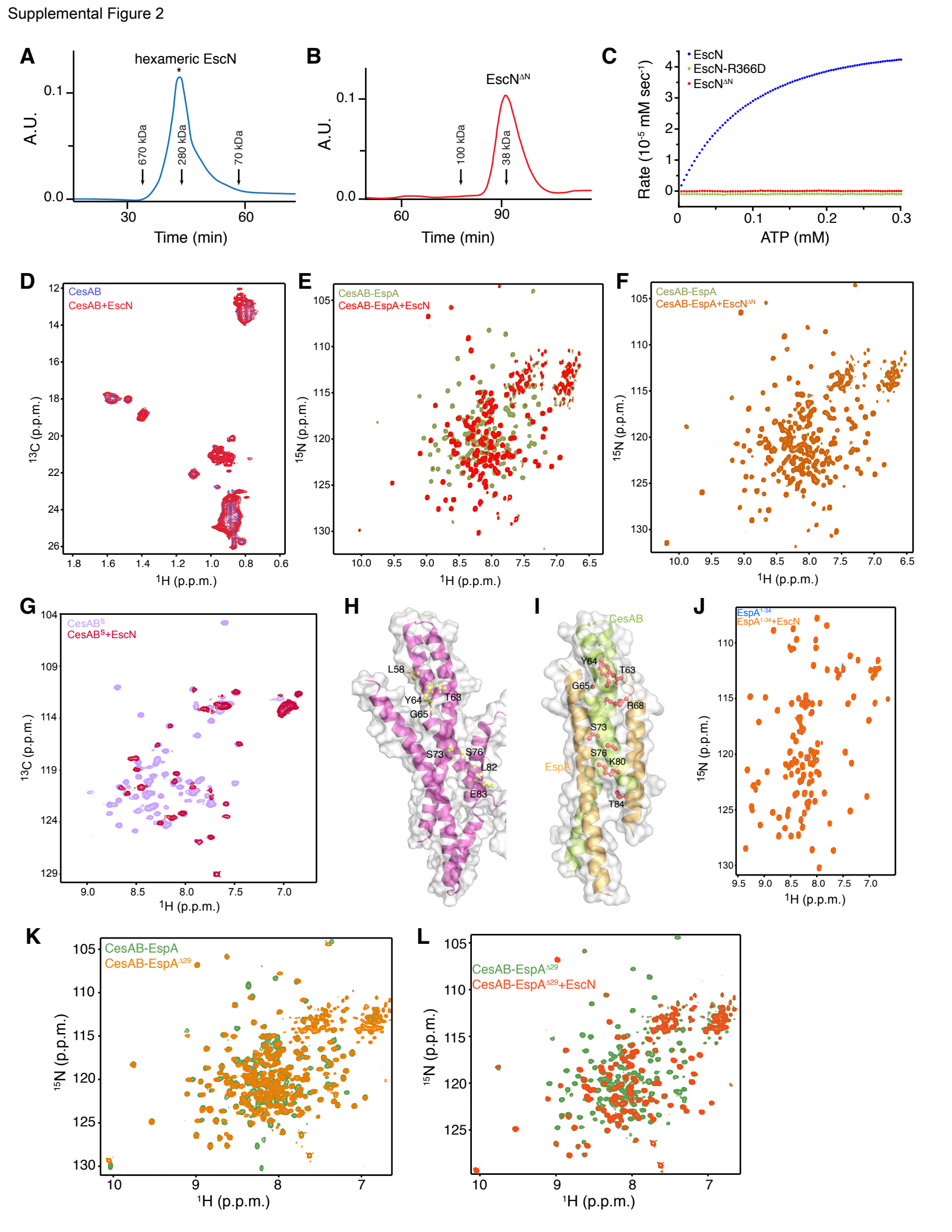

Supplemental Figure 3